# Measurement of Regional Pulmonary Blood Flow with PET

Daniel P. Schuster, James D. Kaplan, Karen Gauvain, Michael J. Welch and Joanne Markham

*Departments of Internal Medicine and Radiology, Institute for Biomedical Computing, Washington University Medical School, St. Louis, Missouri*

We have previously reported a method for measuring regional pulmonary blood flow (PBF) in experimental animals using $^{15}$O-water and PET. The method requires withdrawing blood from the pulmonary artery during the PET scan, so that the input function can be estimated for the one-compartment model used to analyze the data. The purpose of the present study was to modify and validate this technique for a more general use in humans. **Methods:** PBF was measured after injections of $^{15}$O-water in 15 normal subjects and in five patients with reduced cardiac output. In ten of the normal subjects, PBF was also measured after the injection of $^{68}$Ga-albumin macroaggregates (MAA). In the five other normal subjects and in the cardiomyopathy patients, PBF was measured twice after two separate $^{15}$O-water administrations. The input function was estimated from a region of interest (ROI) over the right ventricle (RV), with corrections when necessary, for time delays between RV and lung tissue. **Results:** The mean value for PBF in the normal subjects was 121 ± 32 ml/min/100 ml lung, and was 57 ± 33 ml/min/100 ml lung in the patients with cardiomyopathy. The correlation between PBF measured with $^{15}$O-water and PBF measured with $^{68}$Ga-MAA was r = 0.96. There was no significant difference in the mean value for PBF or the ventral-dorsal distribution of PBF when sequential measurements were made in the same individual. PBF increased in general in the ventral-dorsal direction in these supine subjects, although PBF was more evenly distributed in the cardiomyopathy patients. **Conclusion:** Measurement of regional PBF with $^{15}$O-water and PET appears to be a valid, noninvasive approach for evaluating the pulmonary perfusion pattern of humans.

**Key Words:** positron emission tomography; lung perfusion; blood flow distribution

**J Nucl Med 1995; 36:371–377**

Effective and efficient gas exchange depends upon the close matching of regional perfusion to ventilation. In lung disease, the normal pattern of regional perfusion is often changed, sometimes exacerbating the disturbance in gas exchange (*1,2*). Accurate quantitative measurements of these changes in the regional pattern of perfusion, however, are difficult to obtain in vivo.

We previously reported a method for measuring regional PBF in experimental animals using $^{15}$O-water and PET (*3*). The procedure is a modification of the autoradiographic technique originally described by Kety (*4*), and adapted by Herscovitch et al. and Raichle et al. for use with PET (*5,6*). The method for measuring PBF has been validated against blood flow measurements made with radiolabeled microspheres in animals with normal and low cardiac output (*3,7*).

In the animal laboratory, the water tracer is infused intravenously at a constant rate for 20 sec during a 15-sec PET data collection (*3*). Simultaneously, blood is withdrawn at a constant rate from the pulmonary artery via a previously placed catheter. Time-activity data from these blood samples are used to develop an input function for the one-compartment model that is used to interpret the tissue time-activity data.

Blood withdrawal from the pulmonary artery is impractical for human studies. However, improvements in the spatial resolution of newer PET tomographic scanners makes an accurate estimate of the input function, by obtaining data from a ROI over the right ventricle. Thus, with this modification, we have now measured regional PBF in a group of normal human volunteers and in a group of patients with reduced cardiac function from chronic dilated cardiomyopathy.

## METHODS

The technique for measuring organ blood flow with PET requires an accurate temporal description of tracer concentrations perfusing the lung (input function). Limitations in temporal and spatial resolution with early PET scanners, however, made estimates of right ventricular or pulmonary artery tracer concentrations from ROIs placed over the most appropriate anatomic positions within the heart unreliable, in part due to the short scanning period (15 sec) used to obtain activity data (*3*). This short scanning period was chosen as the best compromise between the desire to maximize counting statistics in the lung tissue ROI on the one hand. On the other hand, the increasing errors in the estimate of PBF anticipated for even small errors in the primary data when the model was applied to data obtained during longer scanning times (*3*). However, inadequate temporal resolution and correction for delays between tissue-activity data obtained by PET and

Received Aug. 1, 1994; revision accepted Nov. 7, 1994.

For correspondence or reprints contact: Daniel P. Schuster, MD, Respiratory and Critical Care Medicine Division, Box 8052, Washington University School of Medicine, St. Louis, MO 63110.

blood time-activity data obtained via a catheter also made direct pulmonary arterial sampling impractical.

As a solution to this problem, the tracer can be administered as a constant infusion, instead of as a bolus, during a PET data collection starting at time $T_1$ and ending at time $T_2$. In such a case, the activity in a tissue region is given by the equation:

$$C_{PET} = C_i \lambda [T_2 - T_1 - (e^{-k_1} - e^{k_2}) \lambda/PBF], \quad \text{Eq. 1}$$

where $k_2 = (T_2 \cdot PBF)/\lambda$, $k_1 = (T_1 \cdot PBF)/\lambda$, $C_{PET}$ is the PET-measured regional tissue activity (counts/100 ml lung), $C_i$ is the input concentration of tracer in blood perfusing the lung (cpm/100 ml blood), $\lambda$ is the regional tissue-blood partition coefficient for water [(ml lung $H_2O$/ml lung)/(ml blood $H_2O$/ml blood)] and PBF is measured in ml/min/100 ml lung. Note that the denominator ml lung in each case includes the contents of vascular, extravascular and alveolar (air) compartments.

To determine $C_i$ in the animal laboratory, blood is withdrawn from the pulmonary artery at a constant rate via a previously placed catheter during scan data acquisition, and the total activity in the syringe, normalized for scan duration and withdrawal rate into the syringe, is taken to be the time-averaged activity of blood perfusing the lung during the scan. If instead, an appropriately placed ROI is positioned within the right ventricle on the PET image, the activity in this ROI would represent the time integral of activity perfusing the lung, analogous to defining the input function by withdrawing blood directly from the pulmonary artery during a constant infusion of activity (*3*). Thus, the same mathematical approach can be used in noninvasive human studies as in the animal experiments.

Regardless of which approach is used to define the input function, additional PET data collection is necessary after the water tracer has equilibrated between the blood and lung tissue. These data are used to calculate an apparent tissue-blood partition coefficient for the tracer ("$\lambda$" Eq. 1). Because tissue density varies throughout the thorax, the apparent lambda will vary accordingly. Again, in the animal laboratory, these data are obtained by referencing lung tissue activity measurements to simultaneously drawn blood samples from the femoral artery. Alternatively, the same ROI within the right ventricular cavity on the PET scan can be used as the estimate of activity in blood.

With this combination of data (lung tissue and right ventricle blood activity during a brief scan immediately after tracer arrives in the lung, and again during a second longer scan to measure lambda after the tracer has equilibrated between lung tissue and blood), regional PBF can be estimated from Equation 1. In all cases, all PET tissue activity measurements are decay-corrected back to the time of isotope administration.

Regional PBF can also be measured after injecting $^{68}$Ga-macroaggregates of albumin (MAA), and this approach was used to help validate the $^{15}$O-water method of measuring PBF. Typically, when organ blood flow is measured with microsphere techniques, blood perfusing the organ is withdrawn at a known rate into a syringe and then regional blood flow is calculated from this simple proportion:

$$\frac{\text{tissue flow}}{\text{syringe withdrawal rate}} = \frac{\text{tissue activity}}{\text{total syringe activity}}. \quad \text{Eq. 2}$$

By using activity in the right ventricle during the scan period instead of total syringe activity, however, the infusion rate can be substituted for withdrawal rate since all activity injected into the antecubital vein will pass through the right ventricle (assuming no loss of activity from the lung because of MAA breakdown during the scan period). Therefore, it is still possible to calculate PBF with radiolabeled MAA noninvasively.

### Isotope Preparation

The technique for producing $H_2{}^{15}O$ has been described in detail previously (*8*). MAA were labeled with positron-emitting $^{68}$Ga ($t_{1/2}$ = 68 min) in a manner similar to that previously described (*3*). Ionic $^{68}$Ga (1137 MBq or 30 mCi) was eluted from a $^{68}$Ga-$^{68}$Ge generator in 3 ml 1 N HCl. The solution was evaporated to dryness under a flow of sterile $N_2$ gas. The residual $^{68}$Ga was redissolved in 200 $\mu$l of 0.1 M HCl as a rinse of the tube. Then, 200 $\mu$l of sterile saline-pluronic-$^{68}$F solution (containing 1 mg/ml pluronic-$^{68}$F in normal saline) was added to a vial of MAA. The MAA solution was transferred to a sterile 12 mm × 75 mm vacutainer tube, and the $^{68}$Ga/0.1 *M* HCl solution was added through a 0.22 $\mu$m filter, followed by 1.0 ml 0.3 *M* acetate, pH 4.75, used to rinse the filter. The tube was then vortexed and incubated for 20 min at 85°C. The solution was then centrifuged at 1800 g to pellet the MAA. The supernatant was removed and the MAA washed three times with 1 ml of saline-pluronic-$^{68}$F solution, prior to final suspension in saline-pluronic-$^{68}$F.

### Data Collection

Data were collected on two different PET tomographs. Before 1993 (the first 10 patients), data were collected on a SUPER-PETT I scanner (*9*). Data was displayed as seven transaxial tomographic slices with a center-to-center separation of 15 mm FWHM and an intrinsic in-plane resolution of 12 mm FWHM. The image reconstruction resolution was 18 mm. After January 1993 (the next 10 patients), data was collected on a SUPER-PET-3000-E scanner (*10*). Data are still displayed as seven transaxial slices, now with a center-to-center separation of 10.5 mm FWHM and an intrinsic in-plane resolution of 8.5 mm FWHM. The image reconstruction resolution was set at 12 mm.

In all cases, a background (blank) scan was obtained, followed by a transmission scan (using a $^{68}$Ga/$^{68}$Ge source) of 10–12 min duration after the subjects were positioned supine in the scanner. (With SUPER-PET I, a ring source of $^{68}$Ga/$^{68}$Ge surrounding the patient was used; with the SUPER-PET-3000-E, a rod source which is rotated around the patient is used instead.) The patients were positioned for optimal imaging of the right ventricle and lungs (Fig. 1).

In all patients, approximately 3700 MBq (100 mCi) $^{15}$O-water was injected in two fractions into an antecubital vein (for an effective dose equivalent of 160 mrem). In patients studied since 1992, approximately 1850 MBq (50 mCi) of activity were first injected by hand over a 10-sec period. (Immediate administration of the entire dose was not possible because of limitations in data through-put from the scanner.) Activity data were collected at the start of the injection in list mode for at least 30 sec. The distribution of this activity in the lungs was proportional to PBF. Patients were asked to hold their breath at end-tidal ventilation for as much of this period as possible. At the end of this period, the second fraction of activity (740–1850 MBq, i.e., 20–50 mCi) was injected as a bolus. Then, 3 min after the initial injection, a second PET data collection was started to measure lambda, lasting 5 min. (The procedure was slightly different in patients studied prior to 1993, primarily because of differences in the scanner and computer support, but as the overall results were similar (see below), they are not detailed here.) To document reproducibility, this procedure of administering the $^{15}$O-water in two fractions was repeated a second time in the patients studied since 1992.

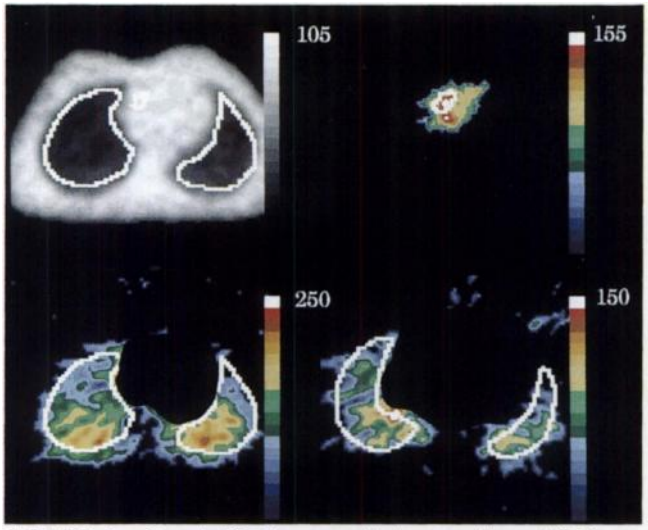


**FIGURE 1.** Sample PET tomographic images. Upper left: Transmission image from one of the normal subjects with lung ROIs shown. Scale is in units of g/100 ml tissue. Also shown is a ROI over the right ventricle. Upper right: Activity from the first 3-sec scan shows significant activity in the field of view, demonstrating primarily activity within the right ventricle (ROI shown). Scale is in units of arbitrary PETT nos/sec/100 ml. The slice position is the same as in the transmission image (the right ventricle ROI is also shown on this image as well). Lower left: Image of pulmonary blood flow as computed from the $^{15}O$ activity data and model (see Methods). ROIs are the same as in the transmission image. Scale is in units of ml blood/min/100 ml lung. Notice the ventral-dorsal increase in blood flow. Lower right: Image of pulmonary blood flow from one patient with dilated cardiomyopathy. Notice lower maximum values than in the normal subject. Also note the reduced ventral-dorsal gradient in flow.

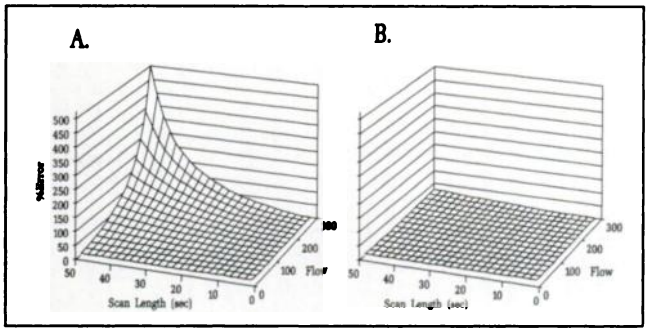


**FIGURE 3.** Results of simulations showing the increasing error in estimating PBF that is encountered for even small (5% underestimation) errors in lambda, especially for long scan lengths, when PBF is estimated in regions of truly high flow or low density (i.e., low lambda). A: True $\lambda = 0.15$. B: True $\lambda = 0.45$.

In patients studied prior to 1993, estimates of PBF obtained from $^{15}O$-water data were compared to PBF calculated from data obtained with $^{68}Ga$-MAA. Approximately 120,000–200,000 particles (up to 46 MBq (1.25 mCi) $^{68}Ga$-MAA) were injected, after dilution with saline pluronic to 15 ml. The MAA solution was injected at 19 ml/min. Again, the scanner data collection was started at the time of injection. Data were collected for 8 min. In this way, all activity moving through the right heart during the approximate 45-sec infusion of MAA was captured (allowing the input function to be estimated). The longer total imaging time generated satisfactory counting statistics for images of the lung regions embolized with MAA.

This study was approved by our institution's Human Studies Committee and the Radiation Drug Research Committee. All subjects gave informed consent to participate.

### Image Processing

The 30-sec list mode data collected during the $^{15}O$-water infusion was processed into consecutive 3-sec frames (Fig. 2). Beginning with the first frames showing a significant increase in activity in the field of view (arrow, Fig. 2), a set of six consecutive frames (18 sec) was combined into a single image. This composite image, then, was used to calculate PBF according to Equation 1. The first frames with activity were also used to locate the right ventricle (Fig. 1).

Eighteen seconds was the chosen scan duration because computer simulations showed that error sensitivity to small errors in the primary data (such as a 5% error in $\lambda$) was small if scan duration was short (Fig. 3). These simulations were performed by computing integrated tissue activity, $C_{PET}$, from Equation 1 with assumed values for scan length ($t_1$ assumed to be zero), flow and $\gamma$. The PBF estimation algorithm was used to estimate PBF from the computed PET activity with correct values for all input parameters except $\gamma$, which was set to 0.95 times the true value of $\gamma$. The

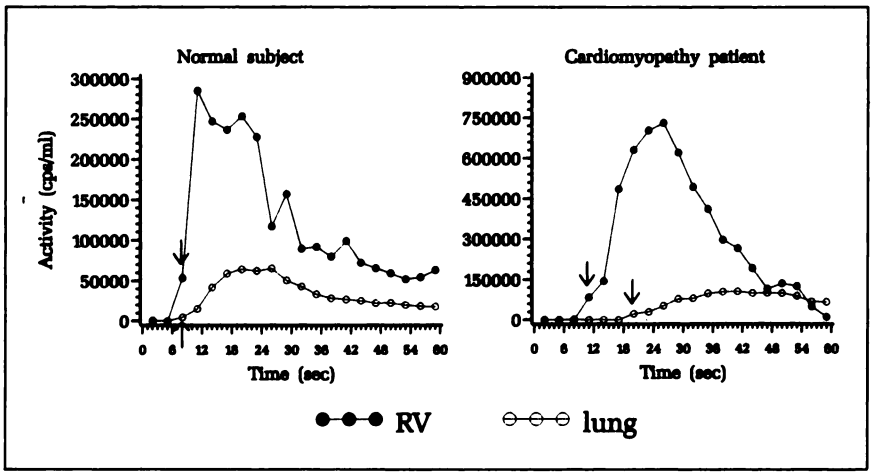


**FIGURE 2.** Time-activity data after the injection of $^{15}O$-water. Each point represents data from a 3-sec scan. Arrows point to the first frame used to determine the beginning of the composite 18-sec scan formed to estimate pulmonary blood flow. Notice the delay in activity reaching the lung tissue region from the right ventricle (RV) in the cardiomyopathy patient.

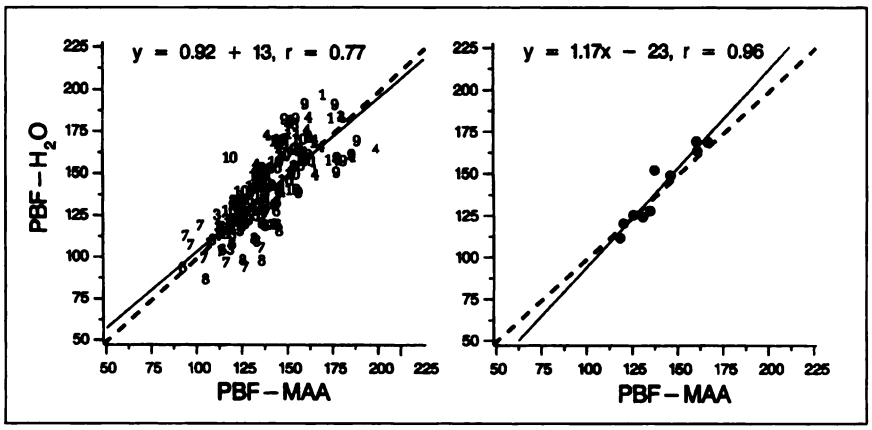


**FIGURE 4.** Correlation of pulmonary blood flow (PBF) estimated from $^{15}O$-water data (PBF-$H_2O$) and from $^{68}Ga$ labeled macroaggregates (PBF-MAA). Left side: Each point represents data from one lung on one of the seven slices (n = 140). Each number represents a single patient (n = 10 patients). Right side: Each point represents the average of all regions for each individual patient (n = 10). Also shown are the regression equations and the correlation coefficient for each case.

estimated PBF was then compared to the true PBF to yield the percent error in PBF due to a 5% error in $\gamma$.

Because activity in the right ventricle preceded activity in tissue regions by more than 3 sec (1 frame) in some cases, especially when flow was low (cardiomyopathy patients), six different frames were used in such cases (Fig. 2, right).

### Image and Statistical Analysis

ROIs outlining both lungs were drawn by hand on four to six slices of each transmission scan and superimposed on the emission images. Care was taken to exclude the chest wall, heart and large vascular structures. The mean value for PBF was then recorded for each region.

As noted above, the first frames of the $^{15}O$-water scan were used to locate the right ventricle, and a ROI was then drawn by hand for placement on the combined image used to measure activity within the right ventricle. The peak pixel value within the region was used. Given the spatial resolution of these scanners, no recovery co-efficient was applied to compensate for possible partial-volume averaging errors (*11*).

For the set of studies obtained since 1992, an additional analysis was employed, as follows. First, the values for all pixels, including their slice number and x-y co-ordinates were transferred as an ASCII file to a computer running the Statistical Analysis System (SAS (R)) software. The PBF value within each pixel was expressed as a fractional flow (PBF/total PBF to the ROI, with the denominator calculated as the mean PBF to the region × region volume, based on voxel dimensions). The data for each region was then sorted, first by the y-coordinate, and then by the x-coordinate into 20 bins, from ventral to dorsal position. Data within each bin were then averaged, and mean values obtained across similarly numbered bins from all regions, within individual subjects, and then within subject groups.

Group data are given as the mean ± s.d. Differences between means were analyzed for statistical significance by a paired t-test (for repeated measures) or an unpaired t-test (for measures between groups). The correlation of PBF values obtained from $^{15}O$-water data versus $^{68}Ga$-MAA data was performed by standard linear regression techniques. All statistical manipulations were performed with the SAS software.

### Subject Groups

The study included a total of 15 normal subjects, including six males who were studied. The age range was 20 to 47 yr. All subjects were healthy, without history of cardiopulmonary disease, and were not taking any medications.

The five cardiomyopathy patients who were studied (including one male) were being evaluated for cardiac transplantation because of global left ventricular dysfunction secondary to a dilated cardiomyopathy. All had an ejection fraction by echocardiogram <25%. Severe left ventricular dysfunction was verified at the time of cardiac catheterization (<1–6 mo prior to the PET study), although cardiac output was actually measured in only one patient. The age range was 41 to 71 yr. Only 1/5 had known coronary artery disease. One patient required continuous dobutamine.

## RESULTS

The mean value for PBF from the normal subjects studied before 1993 was 141 ± 22 ml/min/100 ml lung. The correlation of PBF using either $^{15}O$-water data or $^{68}Ga$-MAA data was excellent (Fig. 4). Regional values showed more variation (not unexpectedly) than overall mean patient values (Fig. 4).

The mean value for the five normal subjects studied after 1992 was significantly higher than the mean value for the patients with dilated cardiomyopathy (Fig. 5). The mean PBF value from the first injection of $^{15}O$-water was not significantly different from the second injection in either subject group. The coefficient of variation between repeat measures of PBF was 7% ± 4% for the normal subjects and 29% ± 33% for the patients with cardiomyopathy. The coefficient of variation for PBF among the regions analyzed in the normal subjects was 10% ± 4% for the first determination and 13% ± 7% for the second. For the cardiomyopathy patients, the values were 15% ± 7% and 18% ± 4%, respectively. A scatter plot of PBF versus lambda is shown in Figure 6.

The distribution of PBF from ventral to dorsal position showed that blood flow generally increased in a gravity-oriented direction, with a small reduction in flow to the most dependent bins (Fig. 7). This distribution was confirmed with data from the second administration of $^{15}O$-water (Fig. 7). However, the overall pattern was more evenly distributed in the patients with cardiomyopathy than in the normal subjects. Sample PBF images are shown in Figure 1.

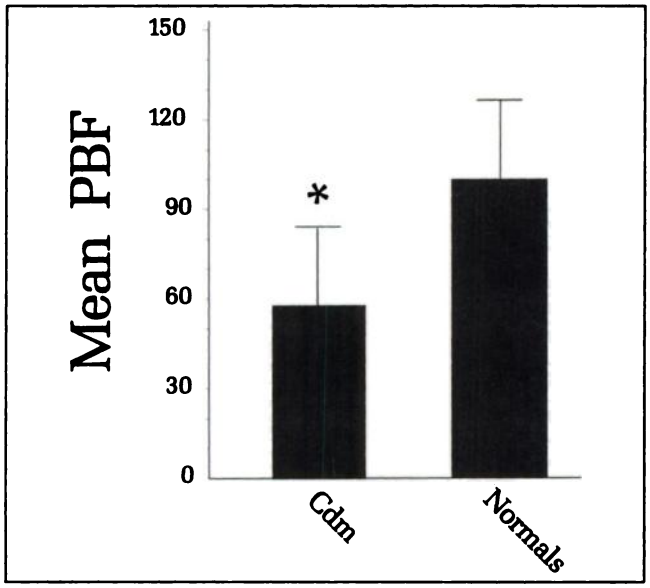


**FIGURE 5.** Mean pulmonary blood flow (average of all regions) ± s.d. as estimated from $^{15}$O-water data, in five normal subjects studied since 1992 and in five patients with cardiomyopathy (Cdm).

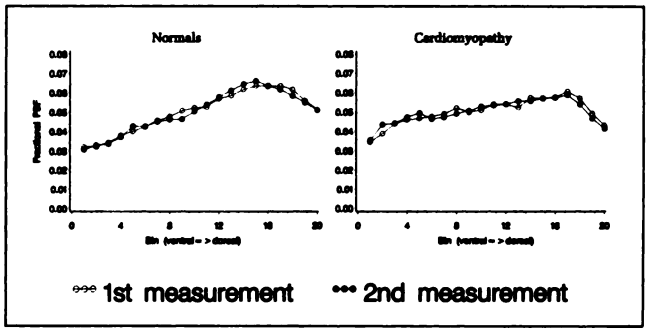


**FIGURE 7.** The mean distribution of pulmonary blood flow along a ventral-dorsal gradient in five normal subjects and five patients with cardiomyopathy. Each curve represents mean data obtained from one PBF determination. Blood flow (fractional flow) is normalized to total flow in the ROI (i.e., mean PBF × region volume, based on voxel dimensions). Each point represents the average fractional flow for like-numbered bins within each ROI on multiple slices in all five patients in each group. Note the increase in fractional flow in normals along the ventral-dorsal gradient in both groups of subjects and the reproducibility of this spatial distribution after a second determination. There is more even distribution of PBF in the cardiomyopathy patients than in the normals.

## DISCUSSION

The classic disturbance of regional PBF occurs after pulmonary thrombo-embolization. However, many studies indicate that the normal pattern of pulmonary perfusion is also altered to varying degrees during states of acute pulmonary edema (*1,2,12,13*). Disturbances in the pattern of pulmonary perfusion may occur as well during other clinical syndromes (e.g., ischemia-reperfusion injury, lobar inflammatory processes) (*14–16*). In humans, regional PBF can be evaluated by radiolabeled MAA, x-ray CT techniques and angiography. However, quantifying the magnitude of changes during disease, especially temporally, or correlating them to other regional physiologic measurements, requires a repeatable, noninvasive technique such as has been described here.

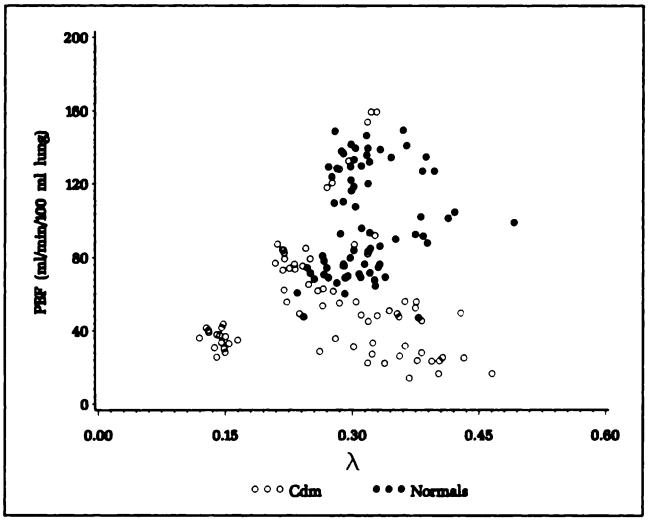


**FIGURE 6.** Scattergram of PBF and lambda in normal subjects and cardiomyopathy (Cdm) patients studied since 1992.

### Technical Issues

The accuracy of the $^{15}$O-water method for estimating regional PBF depends on several factors: (1) the tracer is biologically inert; (2) the tracer exits from a given tissue region in venous blood at equilibrium with the tissue, i.e., the tracer is rapidly and freely diffusible; and (3) the tissue and blood time-activity curves used to estimate PBF can be accurately defined.

All three assumptions have been studied and discussed in previous publications (*3,17*). The results of these previous studies are relevant here as well. In particular, they indicate that the accuracy of the $^{15}$O-water method is particularly vulnerable to errors when lung density is low and flow is relatively high (i.e., $\lambda$ of 0.2 or less when true values of PBF are >2–300 ml/min/100 ml lung). The effect of this combination of conditions is an increasing sensitivity to errors in lambda or $C_{PET}$ (Eq. 1), resulting in overestimations of PBF as lambda decreases and/or true PBF increases (Fig. 3). In this study, however, none of our estimates of regional PBF exceeded 200 ml/min/100 ml lung and values of lambda were in general greater than 0.2 (Figs. 4 and 6).

Thus, we would expect the method to be most reliable during normal or low output states when lung density is normal or high. In contrast, PBF may be seriously overestimated when lung density is very low (e.g., emphysema) or cardiac output is high (exercise or stress conditions). Under such circumstances, PBF could be measured with $^{68}$Ga-MAA as described, although the longer half-life of $^{68}$Ga might make certain experimental protocols impractical.

Markham and Schuster (*17*) also analyzed how errors in

the input function might affect the PBF estimate. In the animal laboratory, an accurate estimate of the input function is achieved by administering the tracer as a constant infusion while blood is withdrawn from the pulmonary artery, also at a constant rate. This procedure allows the input function to be characterized as a step function. In the current study, the first fraction of $^{15}$O-water was injected by hand at a steady rate over 10 sec, yielding shapes which departed somewhat from a true step function, especially in the cardiomyopathy patients (Fig. 2). Departures from this assumption about the shape of the input function will, in general, cause PBF to be underestimated (*17*).

Markham and Schuster also showed that accurate time registration of the input function with the start of scan data acquisition was important. With the procedure reported here, this problem was reduced by acquiring data first in list mode (Fig. 2), so that the arrival of activity could be easily recognized. However, the scan frame lengths were only 3 sec, and even 1 to 2 sec errors may be significant when overall scan lengths are so short (18 sec).

PET is clearly the best currently available method for noninvasively measuring tissue radioactivity in vivo. The principal limitation is the spatial resolution relative to structure size. Activity measurements from the ROI putatively positioned within the right ventricle might be overestimated if some portion of the ROI was actually located within the right atrium. Furthermore, these measurements are the data most likely to be affected by spatial resolution, given the irregular shape and narrow dimensions of the normal right ventricle. Even so, we did not measure a recovery fraction for three reasons:

1. Previous data obtained with the same image resolution as used in the current study (after 1992) indicated that the recovery fraction was >90% in ROIs within the left atrium (*11*).
2. We assumed that the peak value in the RV region would be the value most likely to reflect the true activity within the RV (despite concern about statistical noise for data within any one pixel).
3. Formal validation would require direct blood sampling via a right heart catheter (with risks greater than any benefit for this group of normal or stable volunteers). The actual impact of these assumptions can be evaluated in future studies where a recovery fraction is *actually* measured after blood sampling with a right heart catheter in an appropriate patient population.

Finally, with respect to technical issues, we call attention to the fact that flow was ultimately estimated from the activity in a single 18 sec composite scan, rather than by fitting the model to dynamic data (as in Fig. 2). This approach has several advantages. First, it dramatically reduces the computational time required to produce a flow image, in which flow estimates are made on a pixel-by-pixel basis. Second, we avoid problems encountered by other investigators (such as lower than expected estimates of lambda, despite apparently accurate flow estimates) when applying the Kety compartmental model to dynamic PET data (*18,19*).

**TABLE 1**
Estimates of Cardiac Output, Using PET Measurements of Pulmonary Blood Flow

| Patient no. | PBF (ml/min/100 ml lung) | LTV (ml/100 ml lung) | FRC* (ml) | CO (ml/min) |
|---|---|---|---|---|
| 1 | 94 | 38 | 3910 | 5928 |
| 2 | 72 | 34 | 3150 | 3436 |
| 3 | 122 | 36 | 2950 | 5623 |
| 4 | 131 | 29 | 3110 | 5738 |
| 5 | 72 | 30 | 3050 | 3137 |
| Mean ± s.d. | 98 ± 28 | 33 ± 4 | — | 4772 ± 1364 |

*Based on standard nomograms using age, sex, weight and height.

## Validity

The excellent correlation of PBF estimates by the $^{15}$O-water and $^{68}$Ga-MAA techniques with one another is a test of the mathematical model and other technical aspects of isotope administration, but is not a complete validation of the $^{15}$O-water technique per se since both techniques share some of the same technical features. For instance, time-activity data for the input function were obtained in a similar fashion by both techniques, and both techniques depend on the accuracy of PET to obtain tissue-activity data. On the other hand, the absolute values for PBF can be used to estimate total cardiac output, as follows:

$$CO = [PBF \cdot FRC]/(100 - LTV), \qquad \text{Eq. 3}$$

where CO = cardiac output in ml/min, PBF (ml/min/100 ml lung) is the average value on all slices evaluated, FRC = functional residual capacity (ml) and LTV = lung tissue volume in ml/100 ml lung. LTV was estimated by scaling the transmission scan to the peak soft tissue value (*20*). For each patient FRC was estimated from standard nomograms based on age, sex, weight and height.

Using this approach, we calculated PBF for each of the five normal subjects studied since 1992 (Table 1). The estimates are within the expected range of cardiac outputs in normal individuals. The correlation between PBF and estimated cardiac output was 0.83. Unfortunately, we do not have the actual cardiac output for each person at the time of the PET study as this would have required unjustifiable hazards of cardiac catheterization for research purposes only.

With an additional assumption about blood volume, a similar calculation can be made for the extravascular lung water (EVLW) content of the lung. In four previous studies by several groups (*21–24*), the average blood volume concentration in the lung in normal subjects was 18 ml/100 ml lung, as determined by either $^{11}$CO-labeled erythrocytes or $^{68}$Ga-transferrin and PET. Assuming a similar average value in our normal subjects, the average EVLW concentration would have been 9 ml/100 ml lung (see previous

section). Using the data for LTV and FRC in Table 1, we would calculate an average EVLW content of 434 ml, a value also in agreement with measurements of EVLW by gravimetric techniques (*25*).

The distribution of blood flow shown in Figure 7 is consistent with many previous reports of gravity-oriented increases in blood flow in both humans and experimental animals (*1,26–28*). Interestingly, this gravity-oriented pattern was less pronounced in the patients with cardiomyopathy consistent with the common clinical observation of perfusion redistribution on chest radiographs in patients with heart failure.

Finally, the relatively low coefficient of variation for repeated measures of PBF and the reproducibility of distribution pattern (Fig. 7) suggest that the method will be valuable for assessing the impact of disease or therapeutic interventions on the regional pattern of perfusion.

In conclusion, the data presented in this study support the validity of the $^{15}O$-water estimates of PBF and provides a strong rationale for believing that this noninvasive technique can be used to study regional pulmonary perfusion in humans.

## ACKNOWLEDGMENT

This work was supported by grants from the National Institutes of Health and the Department of Energy.

## REFERENCES

1. Schuster DP. ARDS: clinical lessons from the oleic acid model of acute lung injury. *Am J Respir Crit Care Med* 1994;149:245–260.
2. Pistolesi M, Miniati M, Di Ricco G, Marini C, Giuntini C. Perfusion lung imaging in the adult respiratory distress syndrome. *J Thorac Imag* 1986;3: 11–24.
3. Mintun MA, Ter-Pogossian MM, Green MA, Lich LL, Schuster DP. Quantitative measurement of regional pulmonary blood flow with positron emission tomography. *J Appl Physiol* 1986;60:317–326.
4. Kety SS. Measurement of local blood flow by the exchange of an inert diffusible substance. *Methods Med Res* 1960;8:228–236.
5. Herscovitch P, Markham J, Raichle ME. Brain blood flow measured with intravenous $H_2{}^{15}O$. I. Theory and error analysis. *J Nucl Med* 1983;24:782–789.
6. Raichle ME, Martin WRW, Heroscovitch MA, Mintun MA, Markham J. Brain blood flow measured with intravenous $H_2{}^{15}O$. II. Implementation and validation. *J Nucl Med* 1983;24:790–798.
7. Schuster DP, Marklin GF. The effect of lung injury or alveolar hypoxia on pulmonary blood flow and lung water measured by positron emission tomography. *Amer Rev Resp Dis* 1986;135:1037–1042.
8. Welch MJ, Ter-Pogossian MM. Preparation of short half-lived radioactive gases for medical studies. *Radiat Res* 1968;36:580–587.
9. Ter-Pogossian MM, Ficke DC, Yamomoto M, Hood JT. Design characteristics and preliminary testing of SUPER PETT I, a positron emission tomography utilizing photon time-of-flight information (TOF PET). *IEEE Trans Med Imag* 1982;1:37–41.
10. Ter-Pogossian MM, Ficke DC, Beecher DE, Hoffman GR, Bergmann SR. Design and performance of SUPER PET 3000-E: a positron emission tomograph designed for high count rate, cardiac applications. *J Comput Assist Tomgr* 1994;18:661–669.
11. Bergmann SR, Herrero P, Markham J, Weinheimer CJ, Walsh MN. Noninvasive quantitation of myocardial blood flow in human subjects with oxygen-15-labeled water and positron emission tomography. *J Am Coll Cardiol* 1989;14:639–652.
12. Malik AB, Van Der Zee H, Neumann PH, Gertzberg NB. Effects of pulmonary edema on regional pulmonary perfusion in the intact dog lung. *J Appl Physiol* 1980;49:834–840.
13. Bhattacharya J, Nakahara K, Staub NC. Effect of edema on pulmonary blood flow in the isolated perfused dog lung lobe. *J Appl Physiol* 1980;48: 444–449.
14. Palazzo R, Hamvas A, Shuman T, Kaiser L, Cooper J, Schuster DP. Injury in nonischemic lung after unilateral pulmonary ischemia with reperfusion. *J Appl Physiol* 1992;72:612–620.
15. Hellewell PG, Henson PM, Downey GP, Worthen GS. Control of local blood flow in pulmonary inflammation: role for neutrophils, PAF and thromboxane. *J Appl Physiol* 1991;70:1184–1193.
16. Light RB, Mink SN, Wood LD. Pathophysiology of gas exchange and pulmonary perfusion in pneumococcal lobar pneumonia in dogs. *J Appl Physiol* 1981;50:524–530.
17. Markham J, Schuster DP. Effect of nonideal input function on PET measurements of pulmonary blood flow. *J Appl Physiol* 1992;72:2495–2500.
18. Quarles RP, Mintun MA, Larson KB, Markham J, MacLeod AM, Raichle ME. Measurement of regional cerebral blood flow with positron emission tomography: a comparison of $^{15}O$ water to $^{11}C$ Butanol with distributed-parameter and compartmental models. *J Cereb Blood Flow Metab* 1993;13: 1733–1747.
19. Lammertsma AA, Cunningham VJ, Deiber MP, et al. Combination of dynamic and integral methods for generating reproducible function CBF images. *J Cereb Blood Flow Metab* 1990;10:675–686.
20. Schuster DP, Marklin GF, Mintun MA, Ter-Pogossian MM. PET measurement of regional lung density: I. *J Comput Asst Tomogr* 1986;10:723–729.
21. Schober OH, Meyer GJ, Bossaller C, Creutzig H, Lichtlen PR, Hundeshagen H. Quantitative determination of regional extravascular lung water and regional blood volume in congestive heart failure. *Eur J Nucl Med* 1985;10:17–24.
22. Kaplan JD, Calandrino FS, Schuster DP. Effect of smoking on pulmonary vascular permeability. *Am Rev Respir Dis* 1992;145:712–715.
23. Kaplan JD, Calandrino FS, Schuster DP. A positron emission tomographic comparison of pulmonary vascular permeability during the adult respiratory distress syndrome and pneumonia. *Am Rev Respir Dis* 1991;143:150–154.
24. Brudin LH, Rhodes CG, Valind SO, Wollmer P, Hughes JMB. Regional lung density and blood volume in nonsmoking and smoking subjects measured by PET. *J Appl Physiol* 1987;63:1324–1334.
25. Mihm FG, Feeley TW, Jamieson SW. Thermal dye double indicator dilution measurement of lung water in man: comparison with gravimetric measurements. *Thorax* 1987;42:72–76.
26. Reed JH Jr, Wood EH. Effect of body position on ventricle distribution of pulmonary blood flow. *J Appl Physiol* 1970;28:303–311.
27. Kaneko K, Eilic-Emili J, Dolovich B, et al. Regional distribution of ventilation and perfusion as a function of body position. *J Appl Physiol* 1966;21: 767–777.
28. Glenny RW, Polissar L, Robertson HT. Relative contribution of gravity to pulmonary perfusion heterogeneity. *J Appl Physiol* 1991;71:2449–2452.